Iranian Polymer Journal
12 (5), 2003, 389-400

Mode-II Interlaminar Fracture Toughness of Carbon/Epoxy Laminates

Hossein Saidpour[1], Mehdi Barikani[2(*)], and Mutlu Sezen[3]

(1) School of Engineering, University of East London, Dagenham, Essex, RMS 2AS, UK
(2) Department of Polyurethane and Special Substances, Iran Polymer and Petrochemical Institute
P.O. Box: 14965/115, Tehran, I.R. Iran
(3) School of Design, Engineering &Computing, Bournemouth University, Dorest, BH12 5BB, UK

Received 17 December 2002; accepted 30 April 2003

ABSTRACT

The interlaminar fracture behaviour of unidirectional carbon/epoxy composites has been studied under flexural loading by using end-notched flexure (ENF) specimens. G_{IIc} values were calculated as total fracture toughness energy at the maximum load sustained by the materials as the delamination extended. The results showed that high temperature moulding systems (XHTM45) have the highest G_{IIc} values well above 1000 J/ m^2 . For medium temperature systems (MTM), G_{IIc} has also increased significantly after post cure. For compression strength after impact (CSAI), the behaviour to a certain extent is related to that found for G_{IIc} tests. Comparison of the G_{IIc} values with CSAI also indicated a relationship between two test results. SEM Micrographs revealed their excellent delamination resistance as good crack stoppers with the evidence of strong fibre/matrix interface. Dynamic mechanical analysis (DMA) indicated the increased T_g and modulus retention of the LTM and MTM prepregs after post-curing at elevated temperatures. The failure mechanisms seem to be different for different tough matrix materials and appear to be strongly dependent on the cure and post-curing conditions. This is particularly noticeable for curing at 135°C and 80°C of medium and low temperature moulding systems.

Key Words:
fracture toughness;
carbon/epoxy composite;
delamination;
compression after impact;
end-notched flexure (ENF) test;
unidirectional fibre laminate.

INTRODUCTION

Delamination or interlaminar fracture is one of the major problems for fibre composites. The growth of delamination results in progressive stiffness degradation and eventual failure of the composite structure. The presence of delamination within the composite structure will adversely affect structural integrity, with compressive strength and fatigue performance [1]. So the resistance to delamination is an important composites property of great interest to structural designers [2-4]

(*)To whom correspondence should be addressed.
E-mail: M.Barikani@ippi.ac.ir

Most high performance composites are designed to have superior in-plane strength and stiffness. Such high performance is maintained in cases where the composite laminate has homogeneous and continuous geometry. On the other hand, interlaminar performance is characterized by pronounced weakness under both shear and tensile stresses. Such interlaminar stresses become significant and affect the overall performance where geometrical and material discontinuities exist.

In many composites, the strength reduction has been observed due to delamination between plies. Delamination induced failure is normally a result of a combination of compressive and bending stresses caused by the delaminated plies as they buckle out of plane. The strength reduction in an impact damaged laminate is, however, larger than that caused by delamination of an equivalent size. Therefore, impact damage cannot be represented by delamination alone. Fibre breakage and matrix cracking do have an effect on the strength and a delamination growing out of its plane is not likely to occur unless a considerable fibre breakage occurs. Sometimes the delamination extends to the edge of the material and may grow out of plane without any fibre breakage.

As far as the toughness of composite materials is concerned the low velocity impact damage in carbon fibre reinforced composites (CFRC) has been recognized as a major strength reducing factor [5]. Particularly in aerospace, low velocity impact damage is a result of dropping tools, handling and manufacturing defects, impact from objects and high stress concentration from geometric discontinuities such as free edges, notches, ply termination, bolted or bonded joints. The major reason is that the fibre and matrix are elastic and brittle compared to conventional ductile materials. The failure will initially occur as a matrix cracking followed by splitting between fibre leading to fibre fracture and further delamination can be observed if the bending strains are increased.

Interlaminar shear/tension and the matrix cracking or back surface driven tension failure largely cause the internal delamination which in turn gives rise to residual stresses that further lead to reductions in strength particularly under compressive stresses [6]. The localized damage the so-called barely visible impact damage (BVID) is the potential source of mechanical weakness, particularly under compression loading. The damage pattern is very similar to those observed in laminated plates with open holes under compression loading [7].

Composites with delamination are degraded and need to be carefully examined for safety evaluation. Otherwise, unexpected failure may occur and cause serious damage. In order to design fibre reinforced composites correctly and use them safely, it is necessary to understand the effect of delamination on these materials.

In the recent decade delamination problems have received a growing interest, so many investigations and scientific literature have been involved with interlaminar fracture toughness (IFT) characterization of composite materials [8-13]. The main purpose is to characterize and compare the fracture toughness of different composite systems that consist of unidirectional fibre. The tests measure the energy necessary to produce an interlaminar crack between two plies of a composite material [1].

Many researchers have studied the factors that affect the delamination resistance of composite resin systems and many toughening approaches have been proposed [14]

Several methods have therefore been developed for the measurement of interlaminar fracture toughness under various loading modes. The end-notched flexure (ENF) test [15] is one of the methods designed to measure the interlaminar fracture toughness under in-plane shear deformation mode, commonly known as mode II. The measured G_{IIc} is believed to represent the critical strain energy release rate for crack growth from the insertion film.

In this study an experimental work was carried out on unidirectional carbon/epoxy laminates in order to investigate the interlaminar fracture toughness of ACG40 series prepregs combined with CSAI property evaluation of these materials. An end notched flexure (ENF) specimen is used for deriving IFT under interlaminar shear stress (mode II). In addition to measuring fracture toughness of each system, the mode of deformation and failure were examined using scanning electron microscopy(SEM).

EXPERIMENTAL

Materials

Tests were carried out mainly on ACG40 series of carbon/epoxy prepregs systems such as; HTM40, XHTM45, MTM49-7, MTM49-3 and LTM45-1 offer-

ing toughened laminates with impact resistance. The unidirectional reinforcements used were T800H, IM7 and AS4 carbon fibre with high strain to failure by different manufacturers. These carbon/epoxy prepregs supplied by Advanced Composite Group (ACG).

Instrumental

An Acquati 100DaN tensile testing machine was used for IFT test and fractography was studied by a Phillips 505 scanning electron microscope (SEM). Glass transition temperature was measured by Perkin Elmer dynamic mechanical analyzer (DMA).

Sample Preparation

24 Ply laminates were prepared at 0 ply orientation, with average 60% fibre volume fractions. After the 12^{th} ply, a 16 μm thick PTFE film was placed in the mid-plane to act as a crack starter. In order to ensure laminate quality, debulking was carried out at room temperature after every 4^{th} ply. Following the lay up, laminates were autoclave cured as per the schedules shown in Table 1, followed by the free-standing postcure in an air-circulating oven.

Following cure and post-cure, specimens were cut from the manufactured laminates using a diamond circular saw with a nominal width (B) of 25 mm. The nominal length (L) was 150 mm for G_{IIc} specimens. The edges were polished flat and smooth. Three identical specimens were produced for each specimen design.

Test Methodology

All mode-II tests were performed using a three-point bend, an end notched flexure (ENF). The specimens were positioned in the three-point bend fixture with a total span of 100 mm, so that an initial crack length of 25 mm was achieved. The load was introduced to the specimen by an Aquati 100 DaN testing machine. Mode-II (G_{IIc}) tests were carried out using the in-house method, LIS/MEC/20.

G_{IIc} Tests

In this test, the load was introduced by flexural forces to produce a crack from the insert. The crack then extended as a result of shear forces at the crack tip.

The specimens tested were end-notched flexure (ENF) specimen [1]. The insert (PTFE film) was 50 mm long placed in the mid-plane of the specimen from the edge. The delamination length from the support was α = 25 mm, and total span length was L = 100 mm (Figure 1).

The tests were performed on Acquati using the 100 DaN-load cell. The pre-cracked specimen was loaded in a three point bending fixture at 5 mm/min until the crack propagated. The load applied and the cross-head movement were recorded continuously on chart-recorder and computer. After the maximum load the specimens were unloaded at 50 mm/min. Total fracture toughness energy was calculated from the initial crack length and the load-deflection curve using the highest load (P) and deflection level. G_{IIc} was calculated as [16]:

$$G_{IIc} = \frac{9 \times P \times \alpha^2 \times \delta \times 1000}{2 \times B(\frac{1}{4}L^3 + 3\alpha^3)}$$

where: P is the load (N), δ the displacement (mm), B the specimen width (mm), α the delamination length (mm).

Compression Strength After Impact (CSAI) Test

The aerospace industry has traditionally used drop weight tests on test specimens to explore the nature of impact damage. Tests are normally quoted as the residual compressive strength of the specimen subjected to a predetermined impact.

Over the years CSAI values of various CFRC have been accumulated in an adhoc fashion [17], and the general attitude is that the improvement in damage tol-

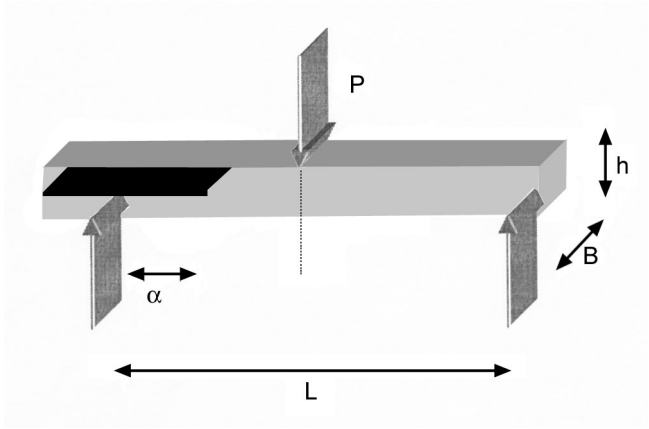

Figure 1. The schematic illustration of the end-notched flexure (ENF) specimen for mode-II(G_{IIC}) testing.

Table 1. ACG40 Series LTM/MTM/HTM composites, thermal and toughness related properties.

Prepreg systems	Cure schedule autoclave	Post-cure (°C)	Reduction in storage modulus (Temp. °C)		Tanδ (°C)	Mode-II G_{IIc} (J/m^2)	CSAI (MPa)
			5%	15%			
HTM40/T800	2h at 180°C	—	—	—	188	1045	223
HTM45/IM7	2h at 180°C	—	177	192	222	1192	—
HTM45/T800	2h at 180°C	—	198	210	235	1097	171.3
MTM49-7/T800	2h at 135°C	—	139	152	196	788.8	86.8
		200	183	192	207	901	103.6
	16h at 80°C	—	92	100	129-207	600	74.9
		135	152	164	192	809.4	143.7
		180	181	189	206	1006	121.3
MTM49-3/T800	2h at 135°C	—	150	168	193	809.4	113.8
		200	162	170	189	1025.5	114.6
	16h at 80°C	—	97	106	124-190	585.3	—
		135	166	176	191	882.6	—
		200	171	179	199	916.9	—
LTM45-1/AS4	16h at 60°C	—	—	—	—	976.9	117.5
		175	167	175	192	868.9	—

erance can be achieved using tougher epoxy resins and high strain fibre.

In our analysis, CSAI was carried out according to SACMA method. Specimens of 150 x 100 mm were cut from 32-ply quasi-isotropic laminates and tested in compression after being impacted at 6.7 J/mm. The CSAI values are also quoted in Table 1.

RESULT AND DISCUSSION

The interlaminar fracture toughness was determined in terms of the mode-II critical strain energy release rate that was regarded as G_{IIc}. All the IFT, CSAI and DMA results including the cure schedule and laminate details are given in Table 1.

G_{IIc} (Mode-II) Test Results

G_{IIc} value was calculated as total fracture toughness energy at the maximum load sustained by the material as the delamination extended. Mode-II interlaminar fracture toughness energy values were naturally higher than mode-I values [18] as expected due to loading conditions that fibres can resist the crack growth better since they are perpendicular to crack opening [19]. All the results obtained from G_{IIc} tests are illustrated in Figure 2. HTM45 showed the highest G_{IIc} values well above 1,000 J/m^2.

After the initial cure G_{IIc} values were fairly low for MTM49-3 and MTM49-7. G_{IIc} for these materials, however, has increased significantly after 200 C post-cure reaching the similar values obtained for HTM materials. This means postcuring conditions have significant effect on fracture toughness energy due to better phase separation and it is necessary for medium and low temperature moulding systems. G_{IIc} values for LTM45-1 laminate on the other hand was not as high as the other 40 series systems.

For the compression strength after impact (CSAI), the values of well above 200MPa were obtained with HTM materials. For the MTM and LTM systems, the compression strength after impact was only increased

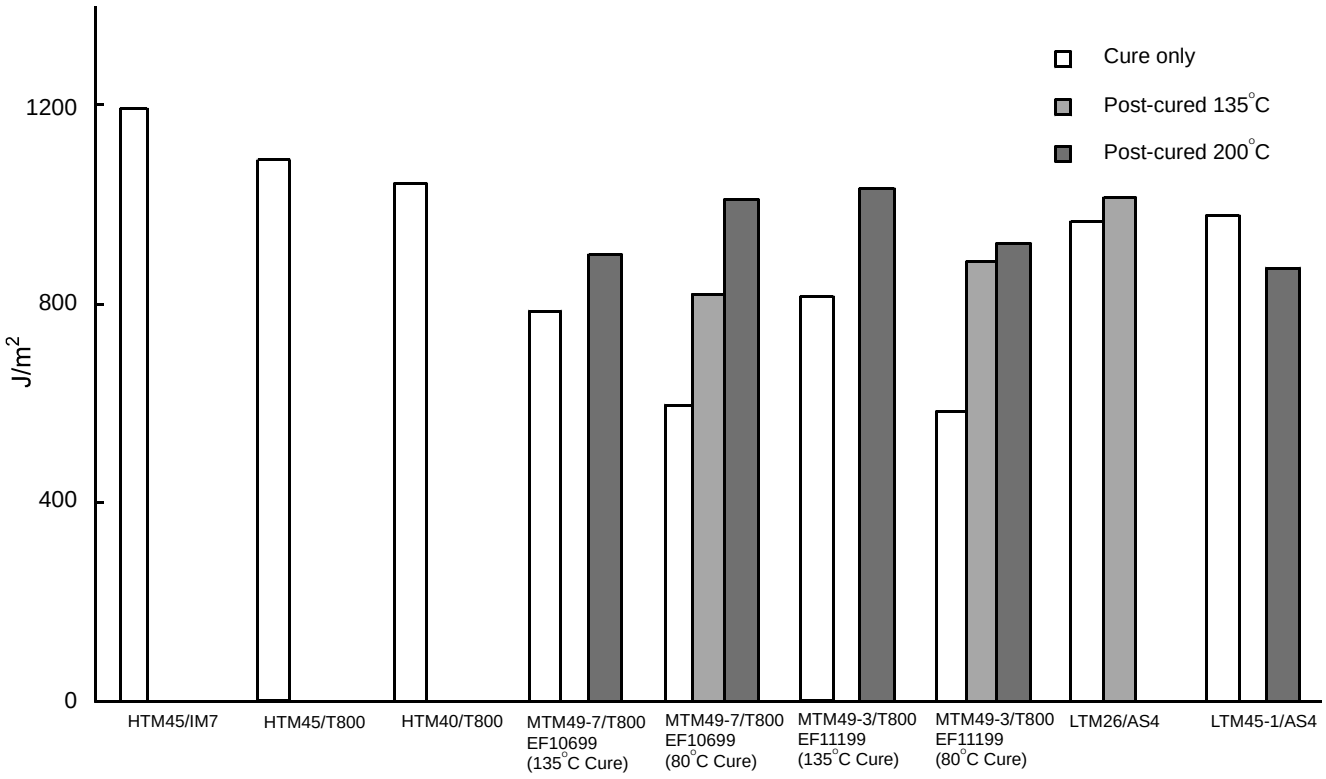

Figure 2. Mode-II (G_{IIc}) interlaminar fracture toughness energy values for all materials.

after the post-cure. Their CSAI was, however, not as high as obtained from HTM materials. The increase after post-cure was also not as much for CSAI as the increase observed in G_{IIc} values. Comparison of the G_{IIc} values against CSAI values in logarithmic form as shown in Figure 3 indicated a relationship between the

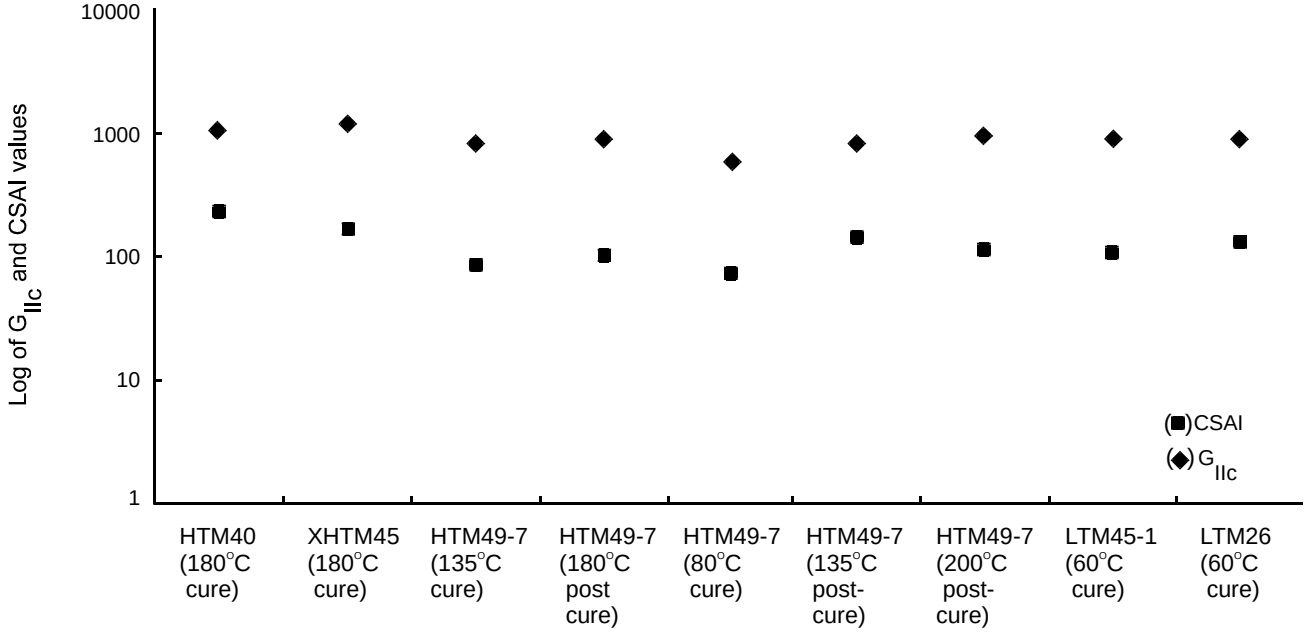

Figure 3. Comparison of the log values of mode-II (G_{IIc}) against compression strength after impact. High fracture toughness related to high CSAI.

two test results.

Fractography (SEM)

All fractured surfaces were subsequently examined in a scanning electron microscopy to determine the degree of resin fracture. The nature of resin fracture (brittle versus ductile) and the degree of microcracking which precedes the fracture were determined by hackles [20] on the fractured surfaces. The SEM micrographs are given in Figures (4-7) .

Different fracture surfaces have been observed after mode-II (G_{IIc}) failure. All the systems exhibited a rougher fracture surface and more hackles were observed than seen in mode-I failure [18]. From mode-II failure, the saw-toothed fracture patterns with rough hackles indicate transverse cracks in resin perpendicu-

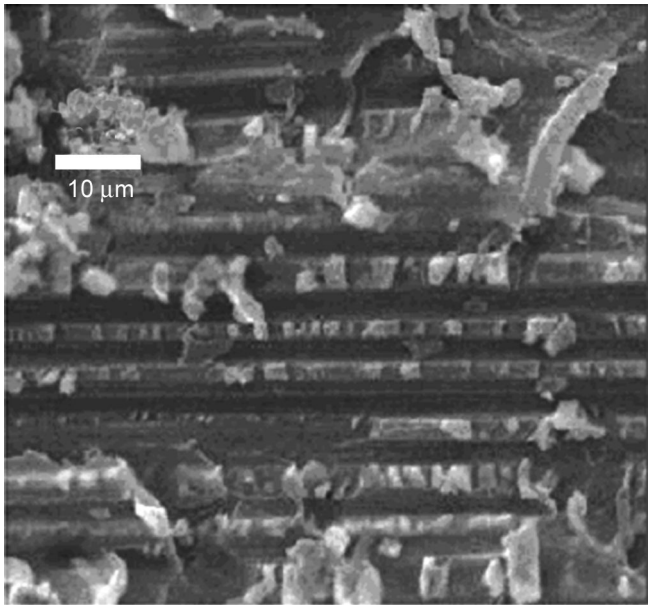

(a) HTM40/T800 180°C/2h

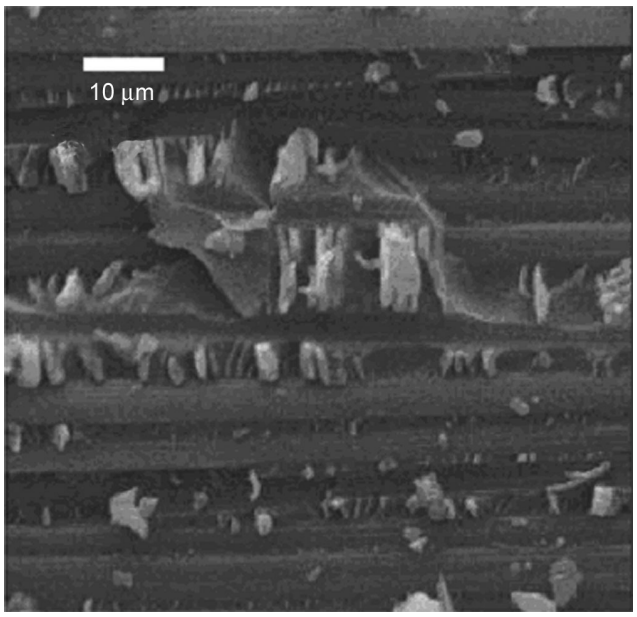

(c) HTM45/T800 180°C/2h cure

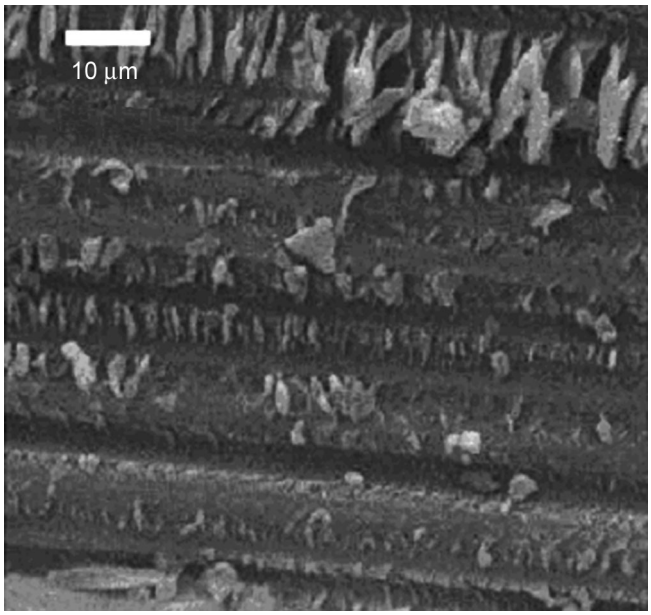

(b) HTM45/IM7 180°C/2h

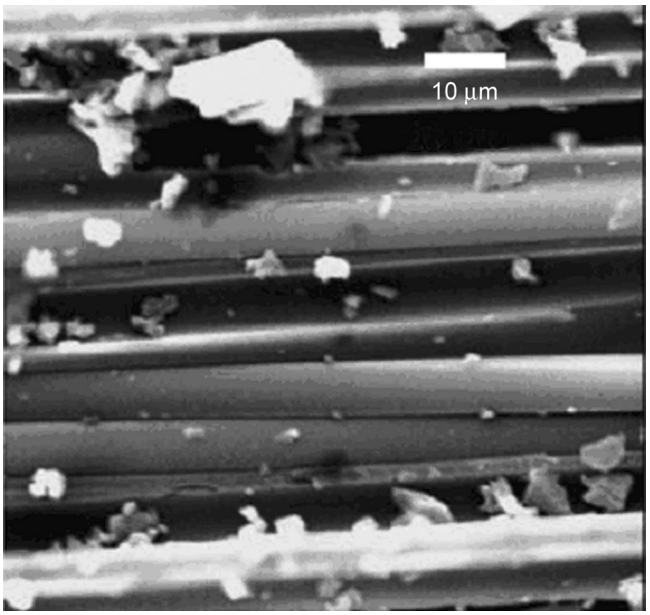

(d) LTM45-1/AS4 60°C/16h + 175°C post-cure

Figure 4. Scanning electron micrographs showing fracture surfaces of HTM 40, HTM 45, LTM 45 composites with different curing systems (X 1000).

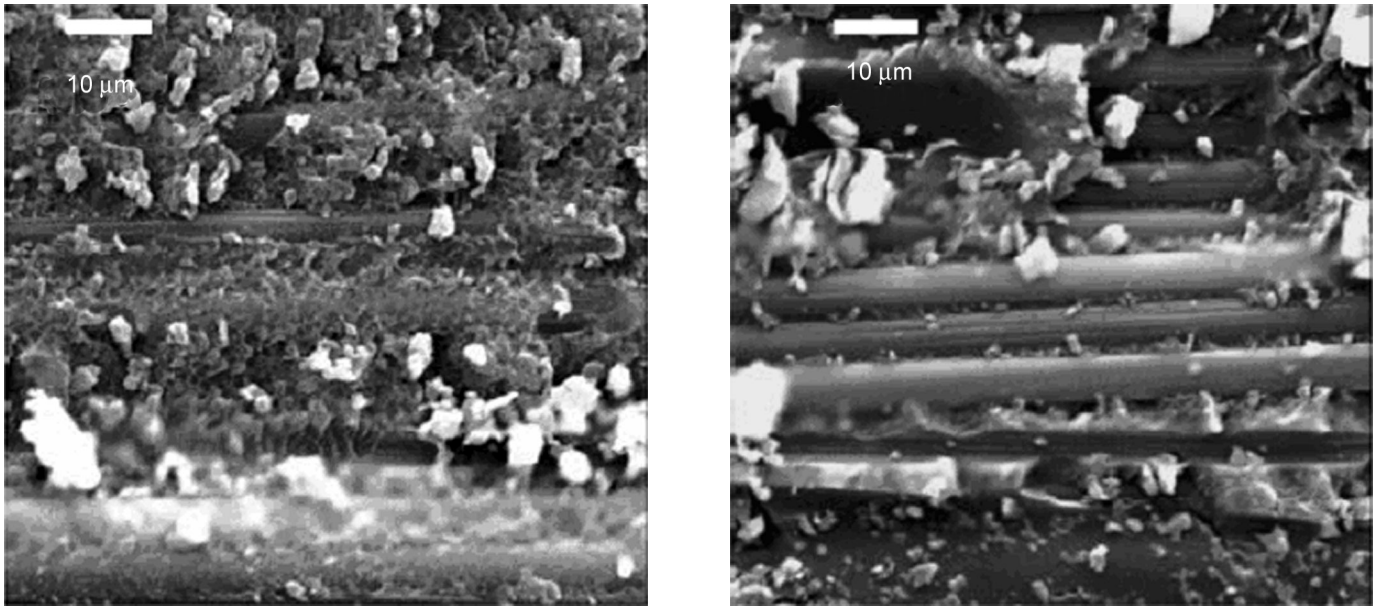

(a) MTM49-7/T800 135°C/2h cure

(b) MTM49-7/T800 135°C/2h + 200°C

Figure 5. Scanning electron micrographs showing fracture surfaces of HTM 49-7/T800 composites with different curing systems (× 1000).

lar to fibres. This correlates with high G_{IIc} results, and shows the material s ability to absorb more energy under mode-II loading.

In the LTM systems after post-cure, the fracture toughness, however, seemed to increase with mode-II shear loading. This increased toughness in the mode-II loading conditions is the result of the microcrack in the resin rich region between the plies on planes perpendicular to the principle normal stresses. Such cracks can only grow a short distance being obstructed by the fibres. This microcracking increases the fracture surface area and results in a more convoluted path for delamination growth. This increase in mode-II fracture toughness was less dramatic in HTM and MTM systems. In the MTM systems where the adhesion was reasonably good, the out-of-plane stress resulting from the shear loading increased moderately. After the 80 C initial cure, the systems did not necessarily show brittle fracture, even more than the ductile failure observed. They neither produced hackle formation after mode-II loading. Thus the fracture mechanism is less affected by a change in loading mode.

In HTM45 system, G_{IIc} was well above 1000 J/m^2. Micrographs also revealed its excellent delamination resistance with elongated hackles. The transverse cracks in resin were perpendicular to fibres (Figure 4). A few resin fractures was at right angle to fibres, then changing direction with resin elongation as the crack propagated. This is a very good way of absorbing energy under shear loading. Thus, HTM45 type is a good crack stopper with high delamination resistance and strong fibre/matrix interface. As well as its improved toughness, HTM45 showed high temperature performance capability with T_g reaching up to 200 C with increased modulus retention at high temperatures shown by DMA graphs (Figure 8).

In HTM40 system, G_{IIc} value was not as high as the HTM45 type. Micrographs from G_{IIc} also showed the strong interfacial adhesion. The hackles occurred due to shear loading indicate the strong resistance of the resin to delamination growth. Nevertheless the hackles were not elongated as much as appeared in HTM45 type G_{IIc} failure. HTM40 is however a tough system with good impact and delamination resistance (Figure 4)

When MTM49-7 cured at 135 C for 2 h, and post-cured at 200 C, the G_{IIc} value improved with post-cure, similar trend was also observed from CSAI values. DMA results showed that the modulus retention was also better after post-curing while T_g increasing up to 192 C (Figure 9).

G_{IIc} Micrographs showed more brittle fracture after 200 C post-cure. Although it showed good transverse crack resistance the fibre debonding was observed during mode-II loading (Figure 5).

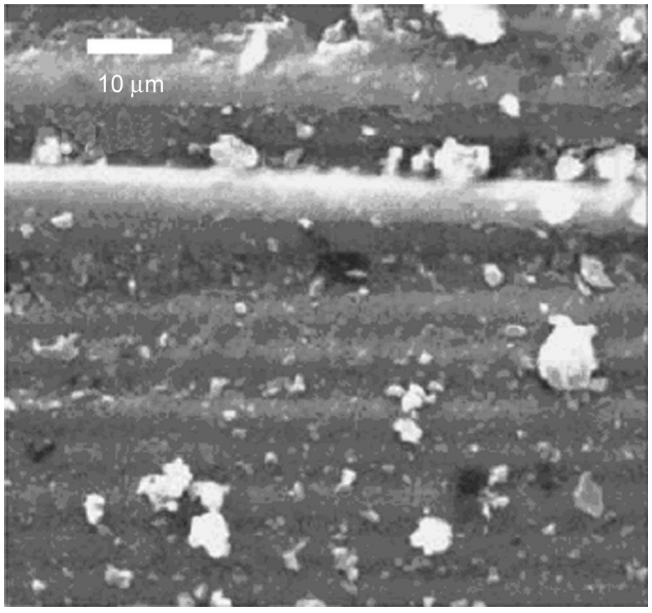

(c) MTM49-7/T800 80°C/16h cure

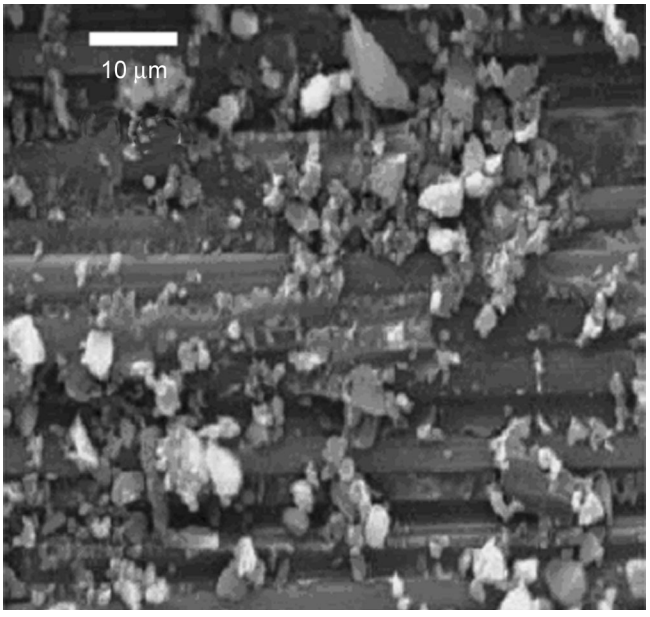

(d) MTM49-7/T800 80°C/16h + 135°C post-cure

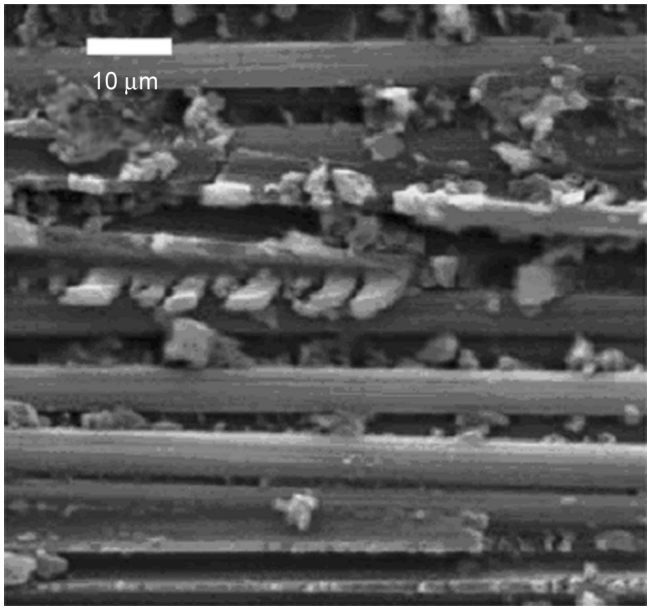

(e) MTM49-7/T800 80°C/16h + 200°C post-cure

Figure 6. Scanning electron micrographs showing fracture surfaces of MTM 49-7/T800 composites with different curing systems (× 1000).

When MTM49-7 cured at 80 C for 16 h, it was evident from DMA traces that at initial 80 C cure the two phases are present and the system is not fully phase separated (Figure 9). The fracture should appear due to the weaker material. As it post-cured up to 200 C, the tan peak indicates the full phase-separation. The storage modulus has also increased with postcure. The G_{IIc} value has also increased, as the material was further post-cured. Micrographs show that the failure became more brittle after the material postcured. The formation of hackles again indicates strong resistance of the resin to delamination (Figure 6). Thus, the delamination resistance of MTM49-7 material increased with post-curing but the interfacial strength was reduced due to internal stress build up during the post-cure. DMA curves showed that MTM49-3 materials are stiffer than

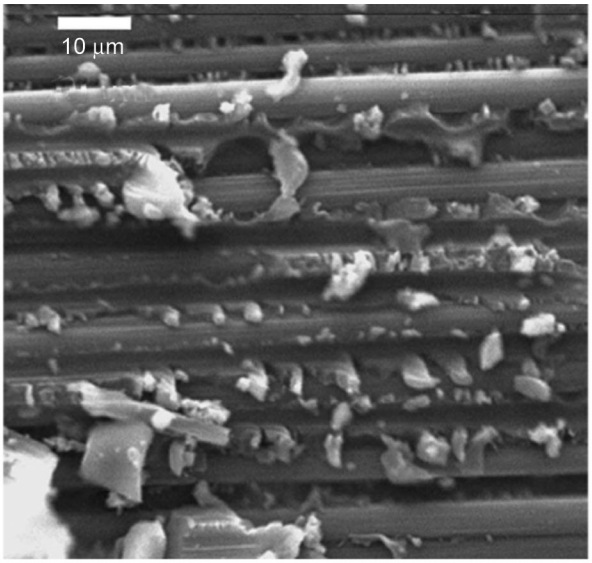

(a) MTM49-3/T800 135°C/2 h + 200°C post-cure

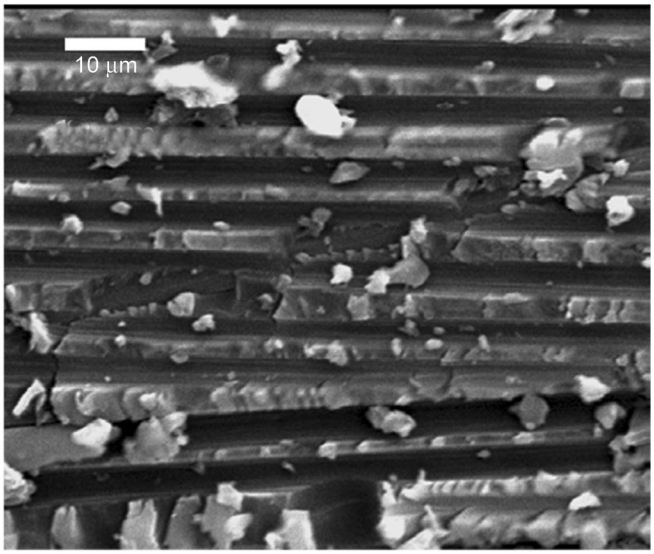

(c) MTM49-3/T800 80°C/16 h + 200°C post-cure

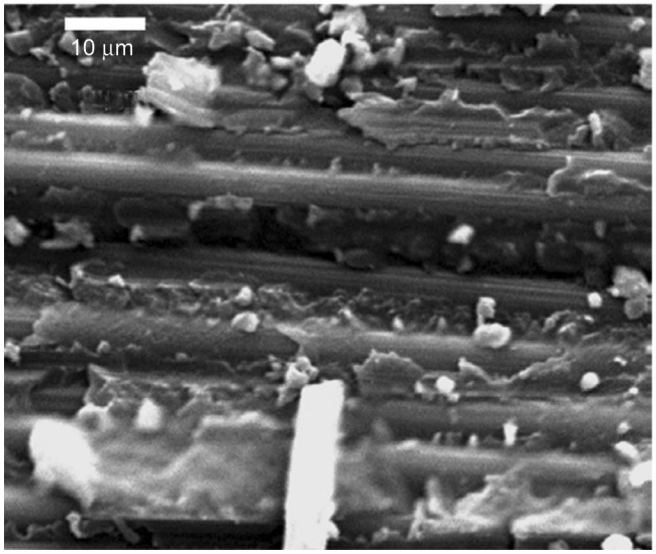

(b) MTM49-3/T800 80°C/16 h cure

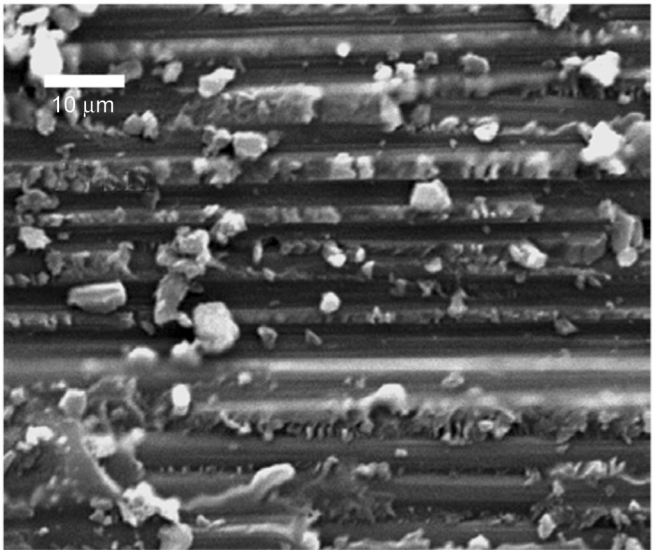

(d) MTM49-3/T800 80°C/16 h + 135°C post-cure

Figure 7. Scanning electron mictographs showing fracture surfaces of MTM49-3/T800 composites with different curing systems (× 1000).

MTM49-7 after the initial cure at 135 C (Figure 10). The reduction in storage modulus initiated much later at 150 C compared to 139 C for MTM49-7 (Table 1).

After the initial cure, the G_{IIc} value of MTM49-3 was higher than the G_{IIc} for MTM49-7 and it has increased after the post-cure similar to MTM49-7, but the level of the increase was higher than increase observed with MTM49-7 G_{IIc} test. The CSAI testing, however, did not show any rise after post-cure. The CSAI values were almost the same.

After 200 C post-cure, more resin fragments were observed and as the fibres failed they left imprints on the resin. Thus the interfacial adhesion was lowered with postcure, but the ability of the material to absorb fracture energy was increased as seen by the strong hackle patterns after G_{IIc} failure. The G_{IIc} fracture pat-

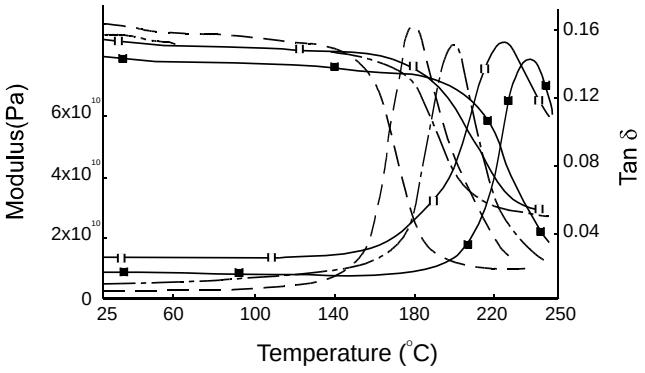

Figure 8. DMA Traces of HTM40/T800 (--); HTM45/T800 (■); HTM45/IM7(□) ; and LTM45 (-.-) systems.

terns of transverse cracks grow along resin perpendicular to fibres after 200 C post-cure. Interesting point is that they grow at right angle along a few fibres, then change direction. This is a very good way of absorbing energy. This shows that although the fibre/resin bond might be low but the toughness was increased (Figure 7).

MTM49-3 was not fully phase separated after curing 16 h at 80 C as two phases appeared on DMA tan δ curve. After the 2 h post-cure at 135 C, a single peak occurred on the tan curve. However, post-curing at 200 C has increased the T_g and the tan δ showed a sharper heating rate (Figure 10).

After the 135 C post-cure, in G_{IIc} failure, the hackles were more apparent showing a mixture of ductile and brittle failures. Thus it should be more resistant to impact damage and crack growth. The 200 C post-cure

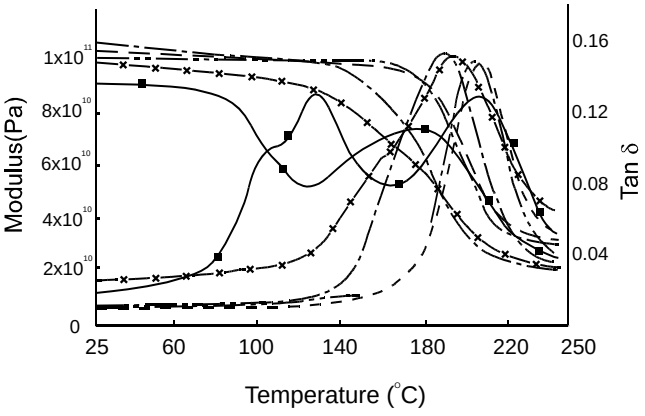

Figure 9. DMA Traces of MTM 49-7/T800 Systems with different curing conditions:
135°C at 2 h (x); 135°C at 2 h + 200°C post-cure(--); 80°C at 16 h (■); 80°C at 16 h + 135°C, post-cure (-.-); 80°C at 16 h + 180°C post-cure (-..-).

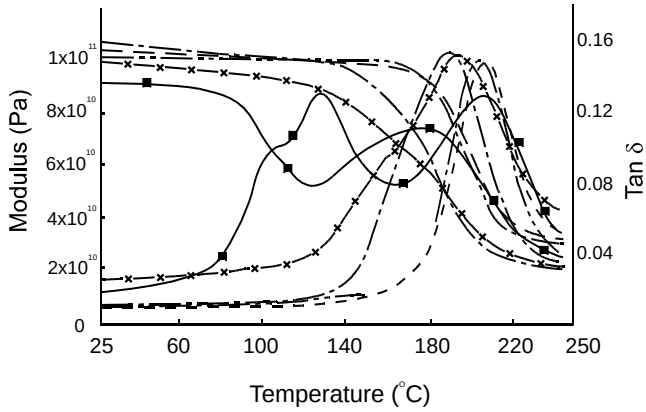

Figure 10. DMA Traces of MTM49-3/T800 systems with different curing conditions: 135°C at 2 h (-); 135°C at 2 h + 200°C post-cure(– - –); 80°C at 16 h (-.-); 80°C at 16 h + 135°C post-cure (-x-); 80°C at 16 h + 200°C post-cure (-•-).

showed sharper hackles, more apparent imprints of fibres as the material failed (Figure 7). G_{IIc} was however lowered compared to 135 C post-cure. The failure was more brittle with some ductile failure.

The G_{IIc} value of 977 J/m^2 for LTM45-1 was by no means low but after post-curing at 175 C was lowered to 869 J/m^2. Although this was lower than G_{IIc} values of other 40 series materials, micrographs showed strong hackle marks that indicate a good crack resistance of the system under shear stresses (Figure 4). DMA tan δ curve indicated the reduction in stiffness appeared after 160 C (Table1).

CONCLUSION

HTM Systems with 180 C cure showed improved toughness in terms of fracture toughness and compression strength after impact property. SEM Micrographs revealed their excellent delamination resistance as good crack stoppers together with the evidence of strong fibre/matrix interface.

When MTM and LTM systems post-cured to elevated temperatures, their mode-II fracture energy was improved, thus it has increased the energy absorption ability of the material. On the other hand, the post-cure is necessary to achieve the high temperature use and complete the cross-linking.

For compression strength after impact (CSAI), the behaviour to a certain extent related to that found from G_{IIc} tests. CSAI values of well above 200MPa were obtained with HTM materials. For the MTM and LTM

systems, the compression strength after impact was also improved with the post-cure at elevated temperatures although their CSAI was not as high as obtained from HTM materials. There are, however, exceptions to the comparable behaviour between the two test methods, such as the increase after post-cure was not as much for CSAI as the increase observed in G_{IIc} values.

Dynamic mechanical analysis (DMA) indicated the increased modulus retention of the LTM and MTM prepregs after post-curing at elevated temperatures. The variations observed in the shape of the tan δ curves after the each post-cure. They could be related to increased toughness performance of the LTM materials. Although they generally showed two T_g s after the initial cure, further post-cure produced single peak tan δ curves and the temperature variation became more symmetrical before and after the peak tan δ values.

The failure mechanisms seem to be different for different tough matrix materials and appear to be strongly dependent on the cure and post-curing conditions. This is particularly a noticeable curing at 135 C and 80 C. However, cure temperature seems to have no adverse effect on the fracture toughness of HTM materials.

ACKNOWLEDGEMENTS

The authors would like to thank the Advanced Composite Group in U.K. for funding this project and for providing the materials. Authors appreciation is given to Mr Majid Barikani for his assistance in type-setting the manuscript.

REFERENCES

1. Compston P., Jar P.Y.B., Burchill P.J., and Takahashi K., The effect of matrix toughness and loading rate on the mode-II interlaminar fracture toughness of glass fibre/ vinyl ester composites, *Comp. Sci. and Technol.*, **61**, 321-333 (2001).
2. Todo M., Jar P.Y.B., and Takahashi K., Initiation of a mode II interlaminar crack from an insert film in the end-notched flexure composite specimen. *Comp. Sci. and Technol.*, **60**, 263-273 (2000).
3. Tsai J.L., Guo C., and Sun C.T., Dynamic delamination fracture toughness in unidirectional polymer composites, *Comp. Sci. and Technol.*, **61**, 87-94 (2001).
4. Albertsen H., Ivens J., Peters P., Wevers M., and Verpoest I., Interlaminar fracture toughness of CFRP influenced by fibre surface treatment: Part 1. Experimental results, *Comp. Sci. and Technol.*, **54**, 133-145 (1995).
5. Jih C.J. and Sun C.T., Prediction of delamination in composite laminates subjected to low velocity impact, *J. Comp. Mat.*, **27**, 684-701 (1993).
6. Jones R., Broughton W., Mousley R.F., and Potter R.T., Compression failure of damaged graphite epoxy laminates. *Comp. Struc.*, **3**, 167-186 (1985).
7. Soutis C. and Curtis P.T., Prediction of the post-impact compressive strength of CFRP laminated composites, *Comp. Sci. and Technol.*, **56**, 677-684 (1996).
8. Hunston D.L., Characterization of interlaminar crack growth in composites with the double cantilever beam specimen. In: *Tough Composite Materials*, proceedings of a workshop held at NASA Langley research center, Hampton, Virginia, May 24-26. :3-17. NASA *Conf. Pub.* 2334 (1983).
9. Kageyama K., Impara I., Ohsawa I., Hojo M., and Kbashima S., mode-I and Mode-II delamination growth of interlayer toughened carbon/epoxy T800H/3900-2) composite systems. In: *Comp. Mat.: Fatigue* and Fracture 5th vol. ASTM STP, Martin R.H., Ed., Phila., 19-37 (1995).
10. Sohn M. and Hu X., Mode-II delamination behaviour of carbon/epoxy composites, Adv. *Comp. Mat.*, **4**, 111-127 (1994).
11. Singh S. and Partridge I.K., Delamination failure in unidirectional carbon fibre/epoxy under mixed mode loading. *Polym. and Polym. Comp.*, **3**, 35-39 (1995).
12. Todo M. and Jar P.Y., Study of mode-I interlaminar crack growth in DCB specimens of fibre-reinforced composites, *Comp. Sci. and Technol.*, **58**, 105-118 (1998).
13. Asp L.E., The effects of moisture and temperature on the interlaminar delamination toughness of a carbon/epoxy composite, *Comp. Sci. and Technol.*, **58**, 967-977 (1998).
14. Groleau M.R., Shi Y.B., Yee A.F., Bertram J.L., Sue H.J., and Yang P.C., Mode II fracture of composites interlayered with nylon particles, *Comp. Sci. and Technol.*, **56**,1223-1240 (1996).
15. Davies P., ESIS protocols for interlaminar fracture testing of composites, France: IFREMER brochure (1993).
16. Gibson R.F., *Principles of Composite Material Mechan-*

ics., McGraw Hill, USA, 395-397 (1994).
17. Pavier M.J. and Clarke M.P., Experimental techniques for the investigation of the effects of impact damage on carbon fibre composites, *Comp. Sci. and Technol.*, **55**, 157-169 (1995).
18. Barikani M. and Saidpour H., Mode I interlaminar fracture toughness in unidirectional Carbon-Fibre/epoxy composites, *Iran. Polym. J.*, **11**, 413-423 (2002).
19. Davies P., Sims G.D., Blackman B.R.K., and Brunner A.J., Comparison of test configurations for the determination of Giic: An international round robin. In: 4th European Conference on Composites: Testing and Standardisation, 31 Aug-2 Sep 1998, Lisbon, Portugal, 161-170 (1998).
20. Morris G.E., Determining fractures directions and fracture origins on failed graphite/epoxy surfaces, *Nondestructive Evaluation and Flaw Criticality for Composite Materials.* ASTM STP 696, 274-297 (1979).